Microstructure and wear properties of FeW-SiC based composite coating produced with Tungsten inert gas (TIG) surfacing method

S. ISLAK*, Ö. ESKİ[a], S. BUYTOZ[b]
Kastamonu University, Cide Rıfat Ilgaz Vocational High School, 37600 Cide-Kastamonu, Turkey
[a]*Kastamonu University, Kastamonu Vocational High School, 37100 Kastamonu, Turkey*
[b]*Firat University, Technology Faculty, Metallurgy and Materials Engineering Department, 23100 Elazig, Turkey*

In this study, SiC reinforced and FeW based metal matrix composite (MMC) was produced on substrate of AISI 304 stainless steel using tungsten inert gas (TIG) surfacing process. In order to examine the effect of SiC on microstructure, hardness and abrasive wear properties inside FeW matrix, SiC was changed by ratios of 10, 25, and 50% by weight. Phase compound and microstructure of coating layers were examined using X-ray diffractometer (XRD) and scanning electron microscope (SEM). Wear behaviours of samples were evaluated using pin-on disc sliding wear tests. It was found that Fe_2C, Cr_7C_3, W_2C carbide and Fe_2Si, $CrSi_2$ silica were formed in the microstructure. The studies conducted concluded that FeW-25 wt. % SiC composite coating was the most appropriate combination in terms of hardness and wear performance.

(Received April 12, 2011; accepted June 9, 2011)

Keywords: TIG coating, Metal-matrix composite, Microstructure, Wear

1. Introduction

Composite coating is generally made up from a ductile matrix and ceramic reinforcement [1]. While nickel, cobalt, iron and titanium based alloys are used as matrix in the production of these composite coatings, in terms of reinforcement elements, hard reinforcement particles such as SiC [2], TiC [3], B_4C [4,5], WC [6,7], TiB_2 [8] and Cr_3C_2 [9,10] are preferred.

In composite coatings, hard particles are reinforced inside matrix in two ways. While in the first method the particle is added to coating layer from outside as mechanical alloying, in the other method reinforcement element is obtained as hard phase inside matrix. This led to formation of a strong metallurgic bond is provided between matrix and reinforcement phase [11,12]. Methods used in the production of these coatings are welding based coating methods [13,14], thermal spraying [15] and chemical and physical vapour deposition [16,17].

Welding based surface coating methods generally include plasma transferred arc, gas tungsten arc, laser beam, submerged, electro-slag and electron beam welding procedures [18,19]. Among the weld cladding procedures, tungsten inert gas (TIG) surfacing process is a cost-effective approach applied when reactive materials (as coatings or substrates) are involved [20]. In this method, substrate surface and powder or hard filler wire used for coating were melted down using arc source and then solidified, which resulted formation of a new composite layer [21-26].

Studies in the literature proved that composite coatings were formed using different powder composites and TIG surfacing method in an effort to a material with better mechanical, physical and chemical properties by making use of another material. Wang et al [27] investigated wearing behaviours of TiC and WC ceramic particle reinforced Ni, Cr, Co, Mo, W, Ti and Cu matrix composite coating that they produced on surface of AISI 1500 steel using TIG surfacing method. Due to the formation of martensite because of rapid cooling rate during coating process and the fact that hard particles make matrix gain resistance, an improvement in wear properties of coating overlay compared to substrate occurred. Lin and et al [28] coated WC:Ti powder composite in 9:1 ratio on AISI 1050 steel using GTA welding method. Conducted examinations demonstrated that a strong metallurgic bond formed between coating overlay and substrate and an increase occurred in hardness and wear resistance due to hard phases.

Xinhong et al [29], having generated TiC phase by using FeCrBSi, FeTi and graphite powder mixtures, produced TiC reinforced metal matrix composite coating. In another similar study, FeTi, FeV and graphite powders mixture were alloyed on AISI 1020 steel by using the TIG coating process [30]. Due to the affinity of Ti and V in making a composite against carbon, TiC and VC carbides formed. And these hard phases contributed increase in the hardness and improvement in wear resistance.

SiC has many advantageous properties such as high melting point (2500°C), high hardness (26.46 kN) and cost-efficient and also be supplied easily as reinforcement phase, particle and fibre-shaped for coating [2].

During conducting this study, aiming to investigate the effect of SiC particles on the microstructure inside FeW matrix, FeW-SiC based composite powders were coated on the surface of AISI 304 stainless steel using tungsten inert gas (TIG) surfacing method. Microstructure characterisation and chemical composition of coating layer

were examined using a scanning electron microscope (SEM), a X-ray diffractometer (XRD), and a X-ray energy dispersive spectroscopy (EDS). Wear behaviours of coatings were interpreted considering micro-hardness measurements and pin-on-disc test.

2. Experimental details

In coating processes, the substrate material used was a 20 mm × 10 mm × 80 mm AISI 304 stainless steel. In order to place coating powders, holes having 8 mm of width and 1.5 mm of depth were drilled on substrates. Before TIG method, surfaces of stainless steel material were cleaned with acetone. In order for shielding gas not to remove metallic powders from the surface of substrate, metallic powders were placed in holes over substrate after being mixed with an amount of bonding. Then, samples were left to dry at 50 °C temperature for 30 minutes. Table 1 illustrates chemical compositions of the powders and the substrate used in coating process.

SiC particles were added to FeW matrix powder in ratios of 10, 25 and 50 % by weight. Size of powder particles are 75 μm on average for FeW, and 40-50 μm for SiC. Table 2 presents composition ratios of coating powders. Fig. 1 illustrates SEM images and EDS analyses of the powders used in coating process.

Table 1. Chemical composition of AISI 304 stainless steel, FeW and SiC powders.

Chemical composition (% weight)	
AISI 304 (Substrate)	
C	0.035
Cr	18.570
Si	0.358
Ni	8.730
Fe	Remaining
SiC powder	
C	27.659
Si	72.350
FeW powder	
W	75.000
Fe	Remaining

Table 2. Composite powders obtained in different SiC ratios.

Sample	Powder ratios	Production speed (mm/s)	*Heat input (kJ/cm)
S_1	FeW-10 wt. % SiC	1.27	42.90
S_2	FeW-25 wt. % SiC	1.21	45.24
S_3	FeW-50 wt. % SiC	1.17	46.80

*Energy input= ηUI(60/1000V); U: voltage, I: current, V: production speed, η: coefficient of performance (0.65 for TIG); [20].

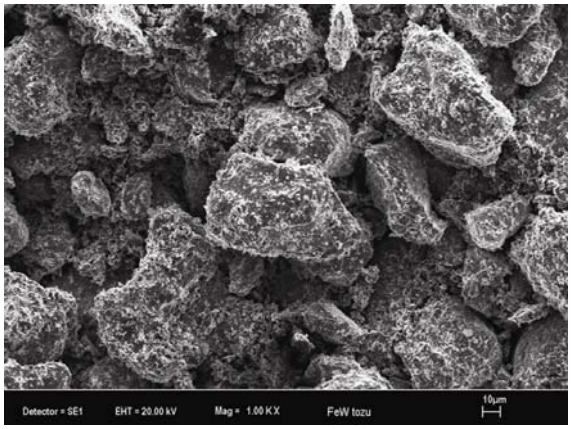

(a)

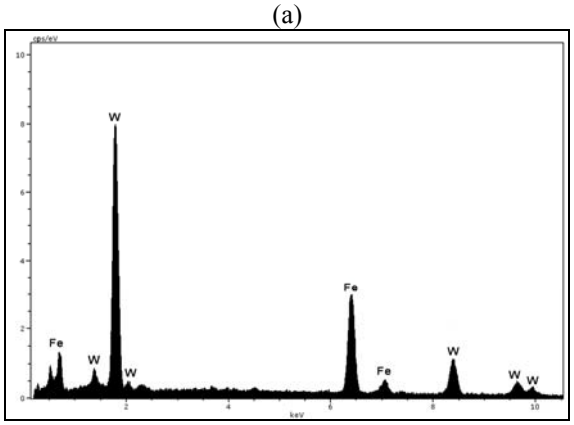

(b)

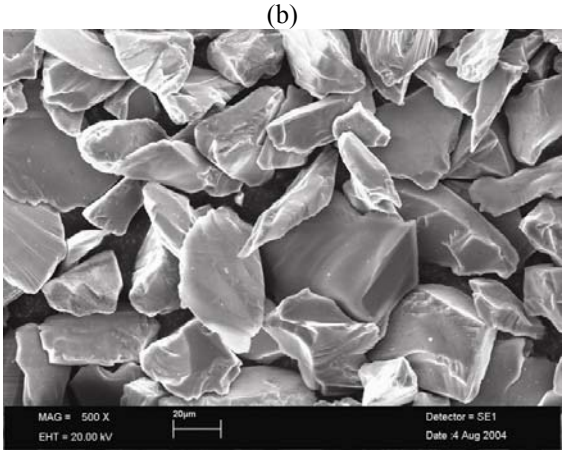

(c)

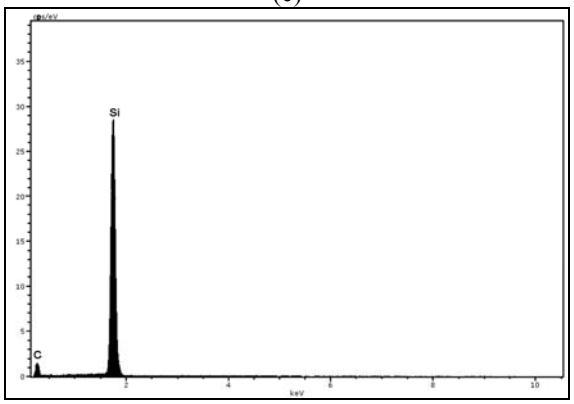

(d)

Fig. 1. SEM image and EDS graphic of metal powders used in coating; (a) SEM image of FeW powder, (b) EDS analysis of FeW powder, (c) SEM image of SiC powder and (d) EDS analysis of SiC powder.

Coating process was carried out using production parameters given in Table 3. Fig. 2 shows principle scheme of surface coating process via TIG.

Table 3. Production parameters.

Electrode	W-%2 ThO_2 electrode
Electrode diameter	2,4 mm
Shielding gas	% 99,9 pure argon
Gas flow rate	12 lt/min.
Current	140 ampere
Voltage	20 V
Production speed	1,17 - 1.27 mm/s
Heat input	42,90 - 46,80 kJ/cm

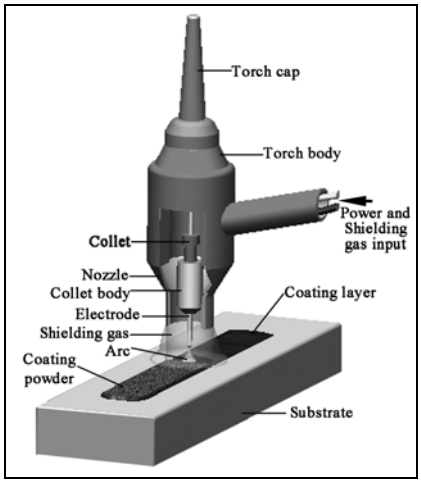

Fig. 2. Principle scheme of surface coating process via TIG.

For microstructure examinations and wear test, 10 mm × 10 mm × 10 mm samples were extracted from middle part of coasting material. Coating materials undergoing metallographic procedures were etched in 5 ml HNO_3 + 200 ml HCl + 65 g $FeCl_3$ solution used as etchant for microstructure examinations. While a scanning electron microscope (SEM) was used for microstructure examinations, X-ray diffraction (XRD) for and X-ray energy dispersive spectrometer (EDS) were used for phase analyses. Hardness measurement were conducted throughout a line from superstrate of the coating through substrate at intervals of 250 μm, in waiting time of 10 sn and with a load of 100 gr using a Future-Tech FM 700 brand micro-hardness device.

Wear experiments of coating samples were conducted with pin-on disc sliding system in room temperature. Experiments were carried out in two different loads of 20 N and 30 N and in sliding distance of 150 m. An abrasive sandpaper of 120 mesh was used. For detecting wear amounts, weight process was performed using an electronic scale of 10^{-4} g precision before and after wear and mass losses were determined. Wear tests were repeated for three times for each sample. Mean of obtained values were taken. After wear rates were measured using the following formula [31-35], and SEM analyses of wear surfaces were carried out, wear performances of FeW-SiC coatings were evaluated. Table 4 illustrates wear test conditions.

$$W_a = \frac{\Delta G}{dMS}(mm^3 / Nm)$$

Where, W_a means wear rate, ΔG is mass loss, M is applied load, d is density and S means sliding distance.

Table 4. Wear test conditions.

Load (N)	20, 30
Sliding distance (m)	150
Counter part material	120 mesh abrasive sandpaper
Temperature (°C)	24
Atmosphere	Dry sliding in air

3. Results and discussion

3.1. Microstructure of coatings

SEM images of FeW-SiC based composite coatings obtained with different SiC reinforcement are seen in Figs. 3-5. SEM image of S_1 sample in Fig. 3 shows that dendrites and inter-dendrite eutectics establish the microstructure. Direction of dendrites is towards the upper area from interface of the coating. The reason for this is absorbing the heat from substrate and also the differences in melting temperature between iron, that is present in SiC and substrate, and other phases [36]

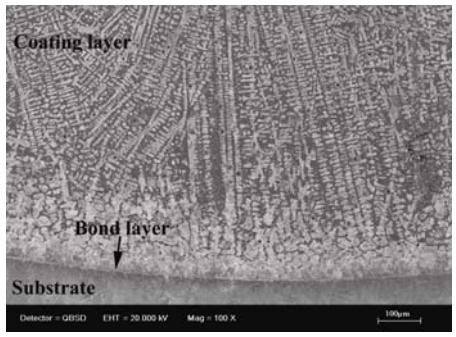

(a)

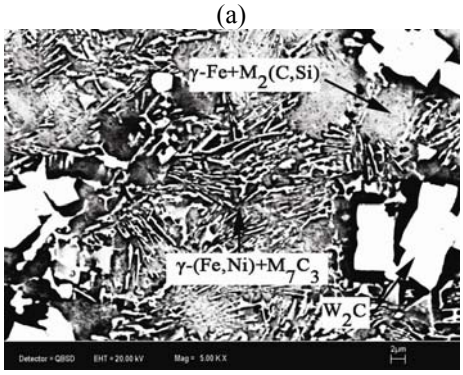

(b)

Fig. 3. SEM image of FeW- 10 %SiC based composite coating (a) general appearance, (b) coating layer.

General EDS analysis of S_1 sample is 3.21 % C, 2.57 % Si, 14.44 % Cr, 4.94 % Ni, 13.21 % W and 61.63 % Fe. EDS analysis of white quadrangle phases seen in Fig. 3b is 13.09 % C, 72.35 % W, 5.44 % Cr and 9.12 % Fe. EDS analysis of rosette phase is 5.21 % C, 7.11 % Si, 6.42 % Cr, 6.28 % Ni and 74.98 % Fe; EDS analysis of reticular eutectic structure is 9.30 % C, 3.61 % W, 17.47 % Cr, 3.68 % Ni and 65.94 % Fe. As observed in EDS analysis and from X-ray diffractogram in Fig. 7, W_2C carbides [37], γ-(Fe,Ni)+M_7C_3 and γ-Fe+ M_2(C,Si) eutectic structures generated in the microstructure of S_1 sample.

Dendritic structure was again observed in the microstructure of S_2 sample coated with FeW- 25 % SiC powder mixture. Undissolved SiC in small quantity was found in coating layer. This situation is also supported with XRD analysis (Fig. 7). This situation demonstrated that the energy given was not sufficient for totally dissolving SiC [38-40]. In S_2 sample, as in S_1 sample, W_2C carbide formed as a result of FeW and SiC powders having been dissolved with the energy given and having been combined with W and C elements, (Fig. 4b).

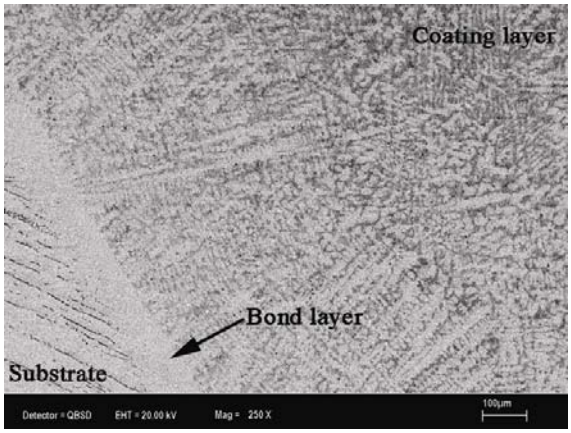

(a)

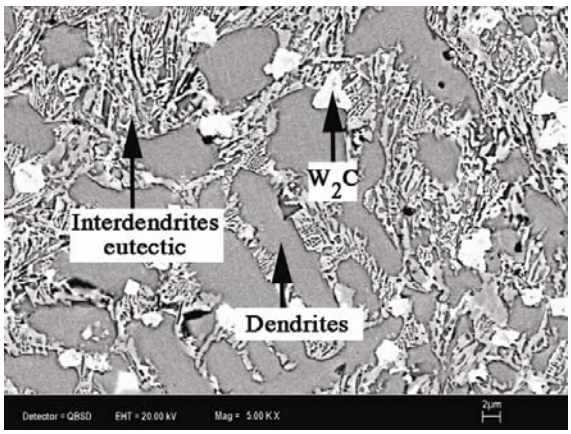

(b)

Fig. 4. SEM image of FeW- 25 %SiC based composite coating (a) general appearance, (b) coating layer.

Fig. 5 presents SEM images of FeW-50 % SiC based composite coating (S_3 sample). Microstructure was formed of dendrites and inter-dendrite eutectics. In this coating, undissolved SiC particles were densely detected. This situation was also detected thanks to the presence of SiC particles on fracture surface (Fig. 6a). Undissolved SiC ratio is higher compared to other coatings (S_1 and S_2). Another observation was that a homogenous metallurgical layer formed between coating layer and substrate (Fig. 6b).

Fig. 7 illustrates X-ray diffractograms of composite coating layers reinforced with SiC. Coating layers generated on the surface of AISI 304 stainless steel samples were made up from γ-Fe, martensite phase ($Fe_{1.88}C_{0.12}$), Fe_2C, Cr_7C_3, W_2C carbide and Fe_2Si, $CrSi_2$ silica.

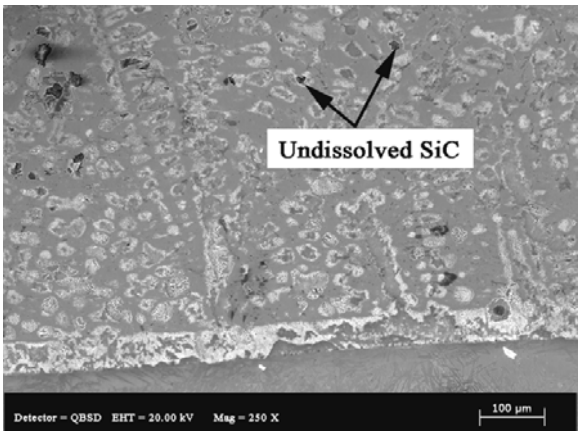

(a)

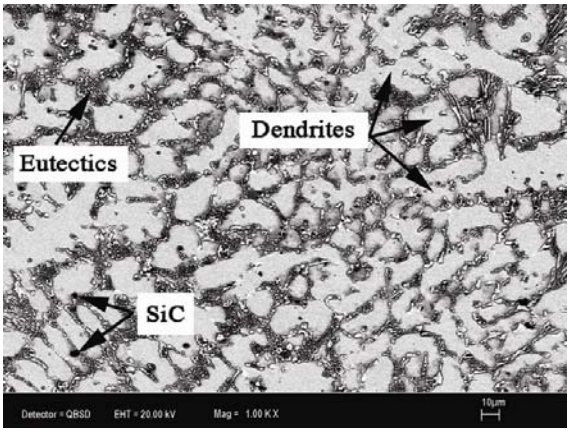

(b)

Fig. 5. SEM image of FeW- 50 %SiC based composite coating (a) general appearance, (b) coating layer.

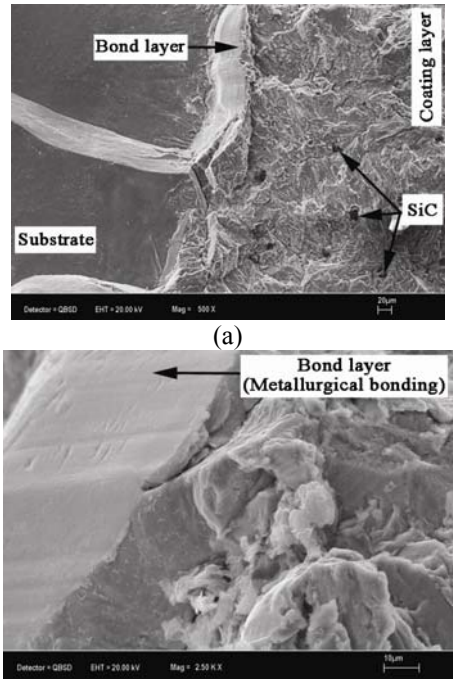

Fig. 6. SEM image of fracture surface in S_3 sample: (a) substrate–interface–coating layer, (b) interface.

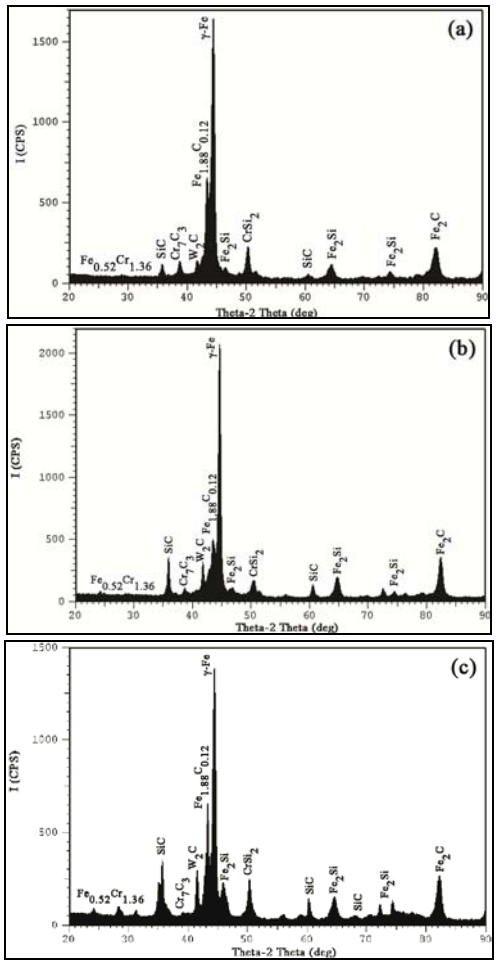

Fig. 7. XRD analysis of FeW-SiC based coatings: (a) S_1 sample, (b) S_2 sample and (c) S_3 sample.

Fig. 8 shows micro-hardness change between coating area and substrates of the samples. Micro-hardness values of FeW-SiC based composite coating samples that were obtained on the surface of AISI 304 stainless steel were measured through a line between a region that is 0.5 mm under coating surface and substrate. It was observed that micro-hardness values were changed depending on amount of SiC powder adding inside FeW powder. Hardness values measured from coating layer of samples are 740, 985 and 435 HV for S_1, S_2 and S_3 samples, respectively. Highest hardness value was observed in sample numbered S_2. The reason behind this is presence of dense Fe_2C, Cr_7C_3, W_2C carbide and Fe_2Si, $CrSi_2$ silica phases in microstructure. While hardness of coating area is in maximum level in the hardness change between coating area and substrate, it reduces in small amount towards interface and reduces dramatically in the interface. This situation is associated with the facts that Fe content is scarce in coating area, and that it is higher in interface area and moreover that density of hard phases in the coating area is high and that this density reduces towards interface and that grains are small in coating area and big towards interface [36,41-43].

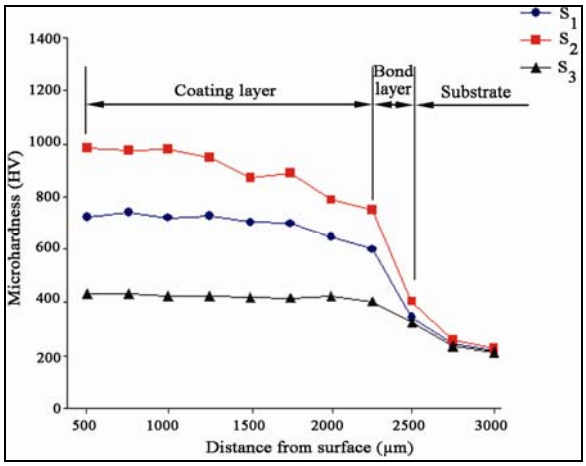

Fig. 8. Micro-hardness graphic from coating layer towards substrate (S_1: FeW - 10 % SiC, S_2: FeW - 25 % SiC, S_3: FeW-50 % SiC).

3.2. Wear behaviour

Fig. 9 illustrates mass loss wear graphics under different loads and depending on distance according to adding amount of SiC powder reinforced inside FeW matrix powder and total wear losses under applied loads. In wear test conducted under load of 20 N, depending on increasing wear distance, the highest amount of mass loss was measured in S_3 sample (FeW-50 % SiC), and the lowest mass loss was measured in S_2 sample (FeW-25 % SiC). Total mass losses under a load of 20 N and in wear distance of 150 m were 0.6218 g for S_1 sample, 0.5352 g for S_2 sample and 0.8785 g for S_3 sample. Total wear losses under a load of 30 N were measured as 0.7434 g, 0.6511 g and 1.1932 g in S_1, S_2 and S_3 samples, respectively. Wear rates illustrated in Fig. 10 were obtained by dividing mass wear loss to applied load, wear

distance and density of wear products. As load per unit surface area increased, wear rate also increased. Despite the increase in silicon carbide (SiC) ratio, the reason behind high wear loss and wear rate in S_3 sample instead of low could be related to the fact that the energy given were not sufficient to dissolve 50 %SiC addition [44]. Hardness of composite coating obtained in this ratio was found lower compared to other coatings. The fact that the most appropriate microstructure design was FeW- 25% SiC was supported by both wear results and hardness measurements.

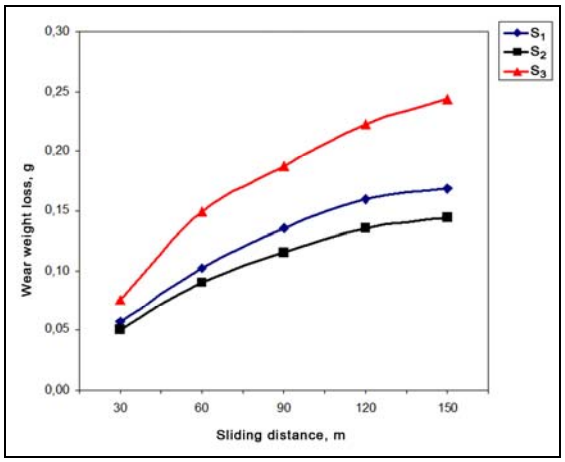

(a)

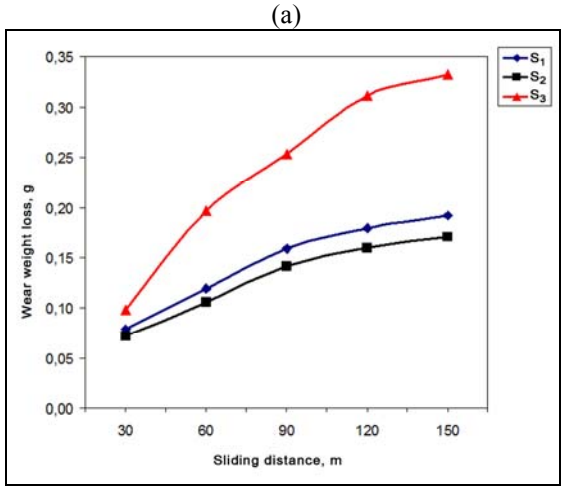

(b)

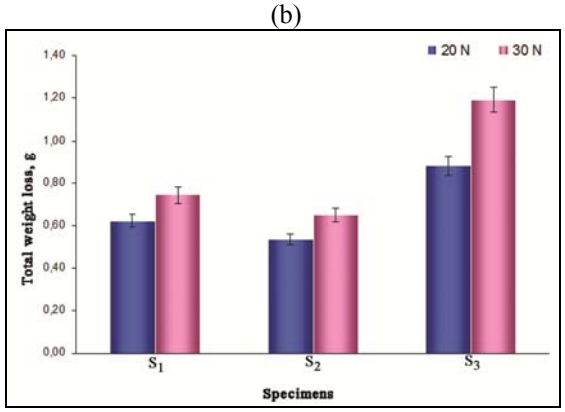

(c)

Fig. 9. Wear losses: (a) under a load of 20 N and (b) under a load of 30 N and (c) total wear losses.

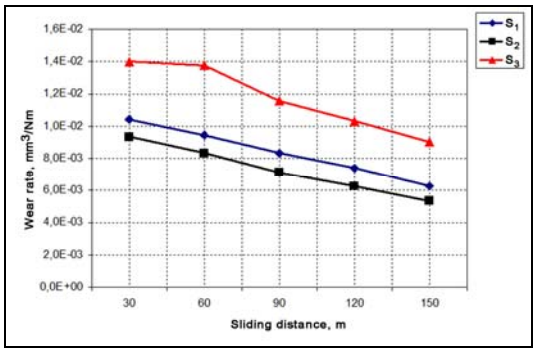

(a)

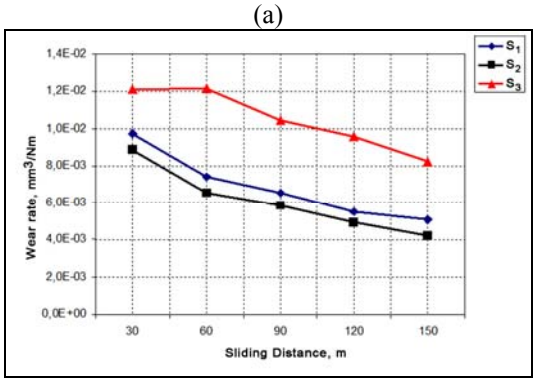

(b)

Fig. 10. Wear rates: (a) Under a load of 20 N and (b) under a load of 30 N.

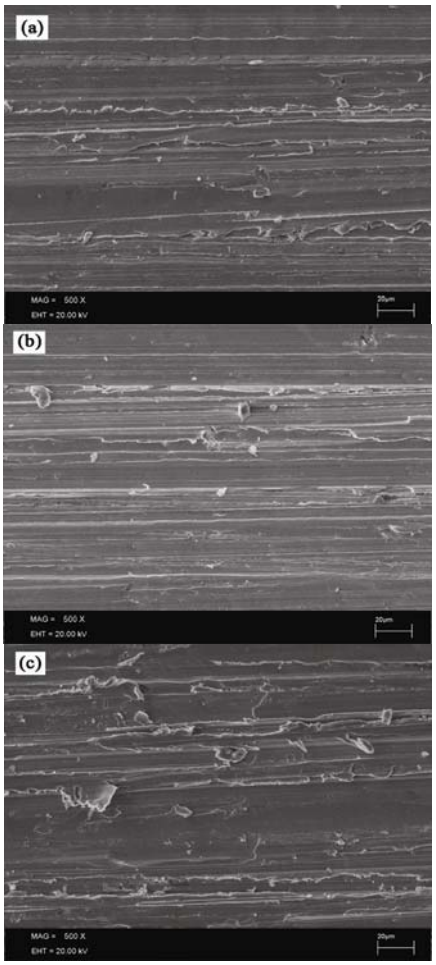

Fig. 11. SEM images of worn surfaces under a load of 20 N (a) S_1 sample, (b) S_2 sample and (c) S_3 sample.

Fig. 11 shows wear surfaces of S_1, S_2 and S_3 samples. As observed from Fig. 11(a) and (b), wear traces were implemented as ploughing. At the same time, grooves are narrow and planar. It was found that surface of S_3 sample from Fig. 11(c) became deformed more during wear and that it was exposed to wear regionally as lashing. Fig. 9 shows that S_3 sample became more deformed compared to two other samples in wear surface detail and that their debris were deeper and hence they were exposed to more mass loss. Its reason is thought to be the presence of undissolved SiC particles inside structure (Fig. 5) and hence that the load coming during wear caused wear as lashing and that it was exposed to more mass loss as result of the fact that load applied in wear distance and undissolved SiC particle were ruptured from coating area due to delamination wear.

4. Conclusions

Microstructure and wear performances of FeW-SiC coatings produced with gas tungsten arc source method were investigated. Conclusions of the study are as follows:

1. Coating thickness was measured as 2-2.5 mm using an optic microscope.

2. Optical and SEM analyses demonstrated that a crack-free and nonporous microstructure formed in these coatings obtained with all production parameters.

3. Coating surfaces were made up from Fe_2C, Cr_7C_3, W_2C carbides and Fe_2Si, $CrSi_2$ silica. Formation of dendritic structures was observed from interface through coating layer.

4. A significant increase was observed in the hardness of FeW-SiC based coatings compared to substrates. Average hardness of the coatings ranges between HV 435 and 985. Maximum hardness value was measured as HV 992 (S_2 sample). The reason behind this is that Fe_2C, Cr_7C_3, W_2C carbide and Fe_2Si, $CrSi_2$ silica phases exist in microstructure densely.

5. Wear performance of S_2 sample were found more excellent compared to S_1 and S_2 samples since the best solution in welding pool with the given energy was obtained in 25 %SiC addition.

References

[1] S. Lu, O. Kwon, Y. Guo, Wear **254**, 421 (2003).

[2] B. Lou, Z. Chen, W. Bai, G. Dong, Transactions of Nonferrous Metals Society of China **16**, 643 (2006).

[3] J. J. Candel, V. Amigo, J. A. Ramos, D. Busquets, Surface and Coatings Technology **204**, 3161 (2010).

[4] M. Chao, X. Niu, B. Yuan, E. Liang, D. Wang, Surface and Coatings Technology **201**, 1102 (2006).

[5] S. Buytoz, M. Ulutan, B. Kurt, S. Islak, İ. Somunkıran, e-Journal of New World Sciences Academy, E-Journal with International Referee 5-1, 35 (2010).

[6] S. W. Huang, M. Samandi, M. Brandt, Wear **256**, 1095 (2004).

[7] G. Xu, M. Kutsuna, Z. Liu, L. Sun, Surface and Coatings Technology **201**, 3385 (2006).

[8] B. Du, Z. Zou, X. Wang, S. Qu, Applied Surface Science **254**, 6489 (2008).

[9] G. Sun, Y. Zhang, C. Liu, K. Luo, X. Tao, P. Li, Materials & Design **31**, 2737 (2010).

[10] Y. P. Kathuria, Surface and Coatings Technology **140**, 195 (2001).

[11] X. H. Wang, M. Zhang, Z. D. Zou, S. Y. Qu, Surface and Coatings Technology **161**, 195 (2002).

[12] A. Singh, N.B. Dahotre, Materials Science and Engineering: A **399**, 318 (2005).

[13] R. L. Deuis, J. M. Yellup, C. Subramanian, Composites Science and Technology **58**, 299 (1998).

[14] B. Gülenç, N. Kahraman, Materials & Design **24**, 537 (2003).

[15] A. Nakajima, T. Mawatari, M. Yoshida, K. Tani, A. Nakahira, Wear **241**, 166 (2000).

[16] J. C. Knight, T. F. Page, Thin Solid Films **193-194**, 431 (1990).

[17] D. E. Wolfe, J. Singh, K. Narasimhan, Surface and Coatings Technology **160**, 206 (2002).

[18] K. G. Budinski, Hardsurfacing: an overview of the process, Welding Design & Fabrication (1986).

[19] W. Wu, L. Y. Hwu, D. Y. Lin, J. L. Lee, Scripta Materialia **42**, 1071 (2000).

[20] K. C. Antony, J. Glenny, J. E. Northwood, Hardfacing, Welding, Brazing and Soldering, Metals Handbook, 9th ed., Vol **6**, American Society for Metals (1983).

[21] Y. C. Lin, S. W. Wang, Tribology International **36**, 1 (2003).

[22] S. Buytoz, M. Ulutan, Surface and Coatings Technology **200**, 3698 (2006).

[23] S. Buytoz, Surface and Coatings Technology **200**, 3734 (2006).

[24] A. W. Orlowicz, A. Trytek, Wear **254**, 154 (2003).

[25] A. Trytek, A. Orlowicz, Archives of Foundry **6**, 319 (2006).

[26] A. Orlowicz, A. Trytek, Archives of Foundry **6**, 313 (2006).

[27] S. W. Wang, Y. C. Lin, Y. Y. Tsai, Journal of Materials Processing Technology **140**, 682 (2003).

[28] Y. C. Lin, S. W. Wang, Yu C. Lin, Surface and Coatings Technology **200**, 2106 (2005).

[29] W. Xinhong, Z. Zengda, S. Sili, Q. Shiyao, Wear **260**, 705 (2006).

[30] W. Xinhong, C. Lin, Z. Min, Z. Zengda, Surface and Coatings Technology **203**, 976 (2009).

[31] M. İzciler, H. Çelik, Journal of Materials Processing Technology **105**, 237 (2000).

[32] M. İzciler, M. Muratoğlu, Journal of Materials Processing Technology **132**, 67 (2003).

[33] M. İzciler, M. Tabur, Wear **260**, 90 (2006).

[34] M. Tabur, M. İzciler, F. Gül, İ. Karacan, Wear **266**, 1106 (2009).

[35] St. Nowotny, A. Techel, A. Muller, W. Reitzenstein, A. Uelze, in: Proceedings of the Fifth European Conference on Laser Treatment of Materials, Bremen-Vegesack, 252 (1994).

[36] G. Thawari, G. Sundararajan, S. V. Joshi, Thin Solid Films **423**, 41 (2003).
[37] S. S. Hua, Y. X Min, L. Y. Yong, H. Y. Zhu, K. Shin, Journal of iron and steel research, International **13-33**, 74 (2006).
[38] X. Wu, Y. Hong, Scripta Materialia **43**, 123 (2000).
[39] X. Wu, G. Chen, Materials Science and Engineering A **270**, 183 (1999).
[40] M. M. Yıldırım, S. Buytoz, M. Ulutan, Practical Metallography **44**, 59 (2007).
[41] L. N. Jian, H. M. Wang, Surface&Coating Technology **192**, 305 (2005).
[42] S. Yang, W. Liu, M. Zhong, Z. Wang, Materials Letters **58**, 1 (2004).
[43] Q. Li, G. M. Song, Y. Z. Zhang, T. C. Lei, W. Z. Chen, Wear **254**, 222 (2003).
[44] X. H. Wang, M. Zhang, Z. D. Zou, S. L. Song, F. Han, S. Y. Qu, Surface and Coatings Technology **200**, 6117 (2006).

*Corresponding author: serkanislak@gmail.com